

Photoinduced Unfolding of β -Lactoglobulin Mediated by a Water-Soluble Porphyrin

John Belcher,[†] Samuel Sansone,[†] Nicholas F. Fernandez,[†] William E. Haskins,[‡] and Lorenzo Brancaleon^{*,†}

Department of Physics and Astronomy, University of Texas at San Antonio, One UTSA Circle, San Antonio, Texas 78249, and Department of Biology, University of Texas at San Antonio, San Antonio, Texas 78249

Received: February 2, 2009; Revised Manuscript Received: March 14, 2009

We investigated the effects that the irradiation of a tetra-anionic porphyrin (mesotetrakis(sulfonatophenyl)porphyrin) noncovalently bound to β -lactoglobulin (BLG) produces on the conformation of the protein. Although BLG is not a potential target for the biomedical applications of porphyrins, it is a useful model for investigating the effects of photoactive ligands on small globular proteins. We show in this paper that irradiation causes a large unfolding of the protein and that the conformational change is not mediated by the formation of reactive oxygen species. Instead, our data are consistent with an electron-transfer mechanism that is capable of triggering structural changes in the protein and causes the Trp19 residue to undergo chemical modifications to form a derivative of kynurenine. This demonstrates that protein unfolding is prompted by a type-III photosensitizing mechanisms. Type-III mechanisms have been suggested previously, but they have been largely neglected as useful mediators of biomolecular damage. Our study demonstrates that porphyrins can be used as mediators of localized protein conformational changes and that the biomedical applications as well as the mechanistic details of electron transfer between exogenous ligands and proteins merit further investigation.

Introduction

Most protein functions, in vivo, are determined by their ability to bind small ligands or portions of macromolecules at specific docking sites. The specificity of these sites is, in turn, controlled by how proteins fold into their native three-dimensional structure. The investigation of the protein structure and folding is still one of the major topics in biophysical research.¹ Photoinitiated events have often been used to investigate the kinetic and thermodynamic parameters of folding/unfolding mechanisms.^{2–5} The use of light to trigger folding changes, however, should not be limited to the basic investigation of how proteins fold. The energy provided by incident photons could be used to prompt conformational changes in proteins with the goal of manipulating their structure (e.g., photoinactivate them). For this type of application the major issue is how to trigger and control the conformational changes in the protein. Recently, a very elegant approach has been introduced that used the photoisomerization properties of azobenzenes.^{6,7} This approach has shown the ability to control the conformation and promote switching between different structures of selected peptides and proteins.^{6,7} Much can be learned from this method; however, since azobenzenes are toxic and carcinogenic,⁸ we have decided to investigate whether another class of photoactive molecules (porphyrins) can be used to prompt protein folding changes. It is known that electron transfer (ET) initiated by porphyrins triggers conformational changes in proteins which contain functional sites for the porphyrins.^{9,10} Porphyrins, however, are also capable of binding several proteins which do not contain specific functional sites for them.^{11–16} Hence, could porphyrins be used to trigger conformational changes in these proteins too? If this was the case, one could use relatively cell-friendly

compounds (porphyrins) to manipulate protein structure. Because of their use as light-activated drugs, the ability to trigger protein unfolding would expand the possibilities for the biomedical applications of porphyrins which traditionally has relied on diffusion-mediated (type I and type II) photosensitization mechanisms which depend on the formation of reactive oxygen species (ROS).^{17–21} The possibility of another mechanism, a type III mechanism,²² has been proposed but its potential role in porphyrin biophysical chemistry has not yet been explored. Type III mechanisms can be summarized as ROS-independent charge-transfer mechanisms, which can produce cytotoxic effects, including protein conformational changes. Because these mechanisms have not been investigated in detail, basic studies are still necessary to understand their potential for biomedical and biophysical applications.

Recently, we have demonstrated that a hydrophobic porphyrin (protoporphyrin IX, PPIX) is capable of inducing partial unfolding of β -lactoglobulin (BLG).²³ As expected for proteins rich in β -structures,²⁴ the photoinduced unfolding was small; however, our finding showed the possibility to use porphyrins to prompt protein conformational changes.²²

In this study, we investigated an anionic porphyrin, mesotetrakis(sulfonatophenyl)porphyrin (TPPS), and found that it induces larger unfolding of BLG. As was the case for PPIX, such changes occur at pH \geq 8 where the protein has undergone its major pH-dependent conformational transition.²⁵ Compared to the previous study, we have now established the likely mechanism that prompts the conformational change and, contrary to what might be expected for porphyrins,²⁶ the unfolding does not appear to be mediated by ROS. Instead, the unfolding is likely to be prompted by ET between the bound porphyrin and the protein which also promotes the formation of a tryptophan (Trp) photoproduct.

Our combined use of optical and protein chemistry techniques yields a possible model for the photoinduced conformational

* To whom correspondence should be addressed. Phone: (210) 458-5694. E-mail: lorenzo.brancaleon@utsa.edu.

[†] Department of Physics and Astronomy.

[‡] Department of Biology.

changes, its triggering mechanism and a quantitative estimate of the unfolding of the polypeptide.

Experimental Methods

Chemicals. TPPS (Frontier Scientific, Logan, UT), and BLG (BLG) (Sigma-Aldrich, St. Louis, MO) were used without further purification. Purity of BLG (>90%) was determined by capillary liquid chromatography–mass spectrometry (LC/MS) and –tandem mass spectrometry (LC/MS/MS).

Buffers. Solutions were prepared in 10 mM phosphate buffer which was adjusted to the selected pH by adding small amounts of 0.5 N HCl or 0.1 M NaOH. The final pH values ranged from 6 to 9 in 1 unit increments. This range spans across the pH of the conformational transition of BLG.²⁷ Because of the substantial dimerization of TPPS at more acidic pH,¹⁴ our investigation was not conducted at pH < 6.

Sample Preparation. BLG and TPPS were dissolved directly into the buffer and their final concentrations were obtained spectroscopically using $\epsilon_{280} = 1.7 \times 10^4 \text{ M}^{-1} \text{ cm}^{-1}$ for BLG and $\epsilon_{413} = 5.1 \times 10^5 \text{ M}^{-1} \text{ cm}^{-1}$ for TPPS.¹²

UV–Vis Absorption Spectroscopy. Spectra were recorded in four-clear-sides quartz cells (NSG Precision Cells, Farmingdale, NY) using a dual-beam spectrophotometer (Evolution 300, Thermo Scientific, Waltham, MA) at 240 nm/min and 2 nm bandwidth. Spectra, corrected for the baseline, were recorded in the 220–350 nm interval for BLG, and in the 350–750 nm range for TPPS.

Emission Spectroscopy. Steady-state fluorescence spectra were recorded using a double monochromator fluorimeter (AB2, Thermo Scientific, Waltham, MA) at 1 nm/s and 4 nm bandpass in excitation and emission. Protein spectra were recorded in the 299–450 nm range upon excitation at 295 nm. Porphyrin spectra were recorded in the 580–750 nm range upon excitation at 413 nm. The optical density (OD) at the excitation wavelength was <0.15 for all samples. Emission intensity, corrected for the instrument response, was calculated by integrating the area under the emission peak and normalized for absorbed radiation according to²⁸

$$F_{\text{corr}} = F_{\text{raw}} 10^{(A_{\text{ex}} + A_{\text{em}})/2} \quad (1)$$

where F_{raw} is raw fluorescence intensity data and A_{ex} and A_{em} are the optical densities of the sample at the excitation and maximum emission wavelength, respectively.

Fluorescence Lifetime. Fluorescence lifetime experiments were performed using a time-correlated single-photon-counting instrument (5000 U, Horiba JobinYvon, Edison, NJ). Fluorescence decay of BLG was recorded upon excitation with a picosecond pulsed source at 295 nm (NanoLED-295, ~700 ps pulse width, Horiba JobinYvon, Edison, NJ) and emission at $330 \pm 4 \text{ nm}$. The decay of the protein was analyzed using the deconvolution software DAS6.2 (IBH, Glasgow, UK). The software yields the value of the fluorescence lifetimes and their relative amplitude through a reconvolution between the time profile of the pulsed source (prompt or $G(t)$) and the theoretical fluorescence decay assumed to be the summation of exponential decays:²⁸

$$F(t) = \sum_i A_i e^{-t/\tau_i} \quad (2)$$

The convolution of $F(t)$ and $G(t)$ is fitted, using a conventional least-squares method, to the experimental decay curve, $I(t)$, by changing the parameters A_i and τ_i .²⁸ The quality of the fitting was ensured by (i) a value of the reduced $\chi^2 \sim 1 \div 1.5$, (ii) the visual inspection of the residuals, and (iii) a value of the

Durbin–Watson parameter between 1.8 and 2.0.²⁹ $G(t)$ was recorded using a 1 mg/mL scattering solution of glycogen in deionized water. Data analysis was carried out with one, two, or three lifetime components and the best fitting that uses the fewer components was chosen.

Circular Dichroism Spectroscopy (CD). CD spectroscopy was carried out using a Jasco J-815 (Jasco Inc., Easton, MD). The secondary structure of the protein was probed in the 190–250 nm range (far UV)³⁰ using 1 mm pathway quartz cells, whereas effects on the aromatic residues (often related to changes in tertiary structure) and in the structure of the porphyrin were probed in the 250–450 nm range,^{30–32} using 1 cm path length quartz cells. The relative contribution of the secondary structure in the 190–250 nm region was estimated using CDPPro.^{31,32} Analysis was carried out using all three fitting procedures offered by the software (SELCON 3, CONTINLL, and CDSSTR) to verify consensus in the fitting parameters.

Capillary Liquid Chromatography–Mass Spectrometry (LC/MS) and –Tandem Mass Spectrometry (LC/MS/MS). Protein identification and characterization by capillary LC/MS and LC/MS/MS was performed in the RCMI Proteomics Core at UTSA. The intact average mass of BLG samples was determined by capillary LC/MS with a splitless nanoLC-2D pump (Eksigent), a 50 μm i.d. column packed with 10 cm of 5 μm o.d. C8 particles, and a time-of-flight mass spectrometer (microTOF; Bruker Daltonics, Billerica, MA, 3–5 ppm mass accuracy and >15 000 mass resolution). Deconvolution of the electrospray charge state envelope, multiply charged $[m + z\text{H}]^{H+}$ protein ions with a mass-to-charge ratio (m/z) corresponding to integral multiples of charge (z), was performed with the maximum entropy algorithm to find the average protein mass (m). The amino acid sequence and modifications of BLG were determined by capillary LC/MS/MS with a splitless nanoLC-2D pump (Eksigent), a 50 μm i.d. column packed with 10 cm of 5 μm o.d. C18 particles, and a with a linear ion trap tandem mass spectrometer (LTQ-XLS; ThermoFisher, San Jose, CA), where the top seven eluting ions are fragmented by collision-induced dissociation (CID) or electron-transfer dissociation (ETD). Probability-based and error-tolerant protein database searching of MS/MS spectra against the NCBI protein database (NCBI nr 20080512; mammalian; 685731 sequences) were performed with a 10-node MASCOT cluster. Search criteria included 1000 ppm precursor ion mass tolerance, 0.8 Da product ion mass tolerance, 3 missed cleavages, semitrypsin, carbamidomethyl cysteines and oxidized methionines as variable modifications, and an ion score threshold of 20.

Irradiation. Irradiation was carried out with a 185 mW, CW laser at 405 nm (Power Technology Inc., Alexander, AR). The laser was defocused and collimated to a 1 cm circular beam. The incident power at the sample was measured at 10 mW/cm² and the samples were exposed for increasing time intervals for a range of doses between 0 and 3.6 J/cm². Irradiated samples included BLG alone and BLG/TPPS complexes. Control samples were of BLG and BLG/TPPS complexes that were kept in solution for the same length of time as the irradiated samples but were not exposed to light until the recording of their absorption, fluorescence, or CD spectra.

Deoxygenated Samples. Oxygen was purged from the solution by flowing pure N₂ (Praxair, Danbury, CT) into an airtight quartz cell (NSG Precision Cells Inc., Farmingdale, NY). Initially the sample was purged with N₂ for 30 min in the dark at which point absorption, emission, fluorescence lifetime and CD experiments were carried out. Subsequently the same sample was irradiated for various time intervals corresponding to the

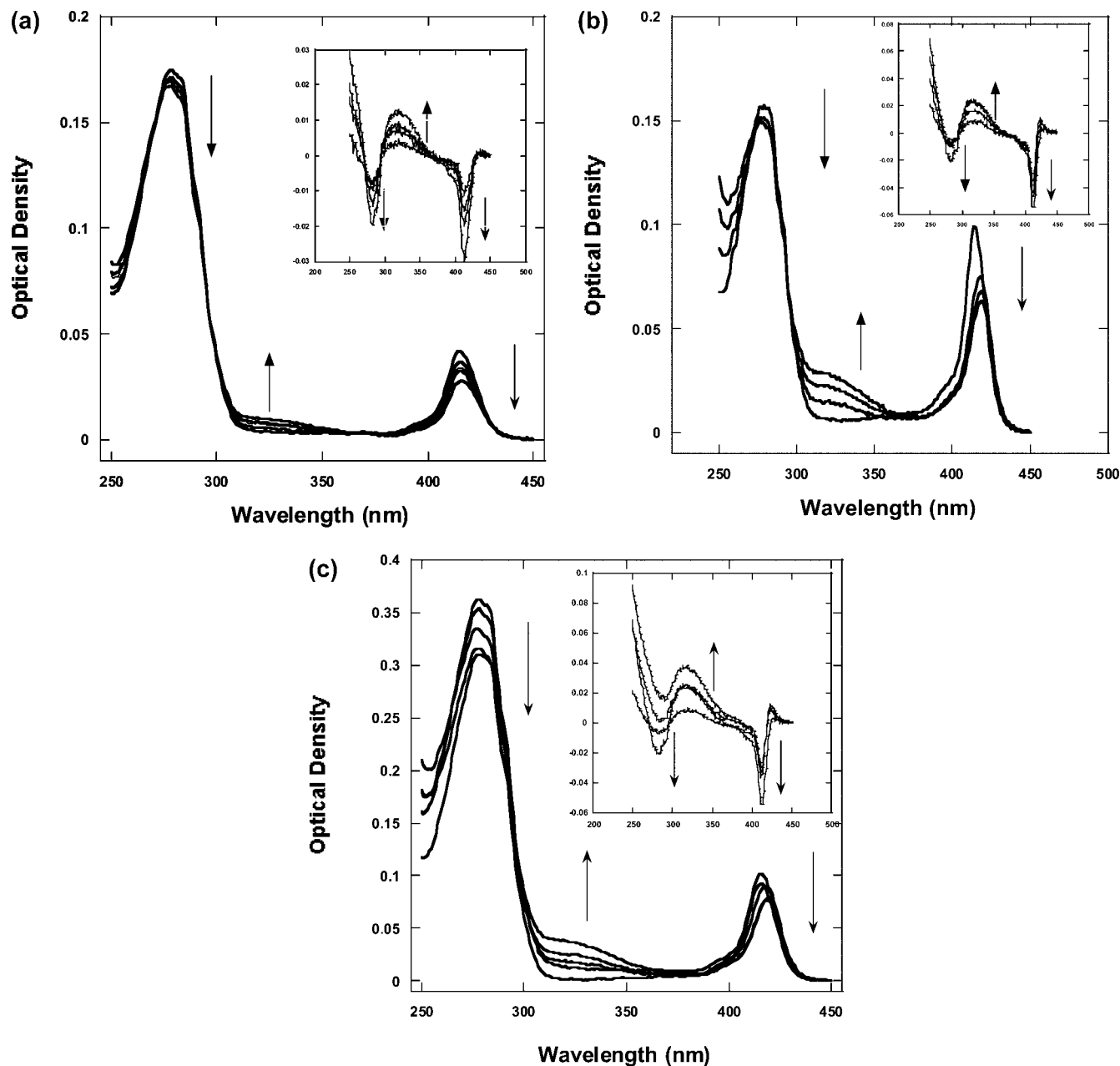


Figure 1. Absorption spectrum of the BLG/TPPS complex as a function of the irradiation energy density (0.0, 0.3, 0.6, 1.2, 3.6 J/cm²). The arrows indicate the direction of the change in absorption as the irradiation increases. (a) pH 6, air-saturated solutions; (b) pH 9, air-saturated solution; (c) pH 9, N₂-saturated solution. The insets show the difference absorption spectra between the complex at increasing irradiation energy density and the nonirradiated complex. Once again the arrows in the insets indicate the direction of the relative change in absorption as a function of the irradiation energy density at the sample. Note that at pH 9 (in air and N₂) the decrease of the band near 413 nm is accompanied by a red shift. The spectra at pH 6 are also representative of the spectra at pH 7, whereas the spectra at pH 9 are representative also of the spectra at pH 8 (Supporting Information).

energy densities above. During irradiation the sample was kept under constant flow of N₂. Thus, the sample was under nitrogen atmosphere before and during irradiation. This avoided the problem of having O₂ reentering the solution during irradiation. After irradiation under N₂ atmosphere the spectroscopic and fluorescence lifetime experiments were repeated.

In order to maintain consistency among different techniques, all experiments (fluorescence, fluorescence lifetime, CD, etc.) were started approximately 20 min after irradiation, since some of the equipment was located in other laboratories. This time lag ensured that the recorded data were not affected by transient, metastable proteins structures.

Results

Irradiation Dependence of TPPS and BLG Absorption.

Irradiation of the TPPS/BLG complex leads to bleaching of the protein (279 nm) and the porphyrin (413 nm). The decrease at 279 nm is accompanied by the increase of a broad shoulder near 320 nm (Figure 1, a and b). At pH ≥ 8 the Soret band of TPPS shifts by ~ 5 nm to longer wavelengths. Since the concentration of TPPS was low (~ 1 μ M), the Q-bands were not clearly visible, and therefore the effects of irradiation in this region was investigated by using fluorescence excitation spectra but they did not reveal any additional information other than a shift of the lowest energy Q(0,1) band (Supporting

Information). The relative bleaching of BLG and TPPS is larger for increasing pH values (equal amount of photon energy density (J/cm^2) deposited in the sample). The increase of the shoulder at 320 nm is twice as large at pH 8 and 9 than at pH 6 (Figure 1b). At alkaline pH but not at pH 6 and 7, the bleaching of TPPS is accompanied by a shift in the Soret band (Figure 1b).

Deoxygenation of the BLG/TPPS solutions did not prevent bleaching of either the porphyrin or the protein, or the formation of the band at 320 nm. As Figure 1c shows, at alkaline pH (but the same applies at pH 6 and 7) the features recorded in the air-saturated samples are still present in deoxygenated samples and the extent of the relative changes observed is comparable to that for samples in air.

Irradiation Dependence of TPPS Steady-State Fluorescence. The bleaching of TPPS (Figure 1) is the reason for the decrease in its emission intensity. However, at $\text{pH} \geq 8$ the photobleaching is accompanied by a 5 nm shift of the $Q(1',0)$ emission maximum to longer wavelengths (Figure 2). Such additional shift is similar, in magnitude, to the one observed in the absorption (Figure 1b) and excitation spectra (Supporting Information). In deoxygenated samples, irradiation produce effects similar to the ones observed in the presence of oxygen in the emission spectra of the TPPS/BLG complex.

Irradiation Dependence of UV Fluorescence (BLG and Products). The irradiation-induced bleaching of BLG in absorption (Figure 1) is responsible for the decrease in the emission intensity of the protein in the TPPS/BLG complex (Figure 3, a and b). However, at $\text{pH} \geq 8$ the decrease in intensity is accompanied by a very slight red shift (~ 2 nm) in the emission maximum which may indicate small changes around the Trp residues.

We investigated the emission properties associated with the irradiation-induced 320 nm shoulder (Figure 1). Excitation of this band produces a broad and weak emission centered near 408 nm (Figure 4, a and b). The low intensity of such band is due to a combination of the small OD and, possibly, a smaller fluorescence quantum yield of the emitting molecule. However, as Figure 4 shows, in agreement with absorption (Figure 1) the emission intensity of this band at alkaline pH is larger than at pH 6 and 7. The excitation spectrum associated with the 408 nm broad peak produces a component of the protein with peak at 279 nm and a shoulder at 321 nm similar to the absorption spectrum (Supporting Information).

Purging the solution with N_2 does not affect the steady-state emission of BLG in the complex upon laser irradiation. The protein is bleached while the maximum of the emission of BLG remains unaffected at low pH and shows the same slight red shift at higher pH values. The emission and excitation properties of the 320 nm shoulder also remain unaffected (Supporting Information).

Intrinsic Fluorescence Lifetime of the Protein in the BLG/TPPS Complex (Air Saturated). Measurements of the fluorescence lifetime provide additional important information regarding the effects of irradiation. In agreement with our previous results,³³ at all pH values, BLG fluorescence decay can be separated into three pH-dependent components.

Irradiation of the samples at $\text{pH} \leq 7$ does not affect the emission decay of the protein in the BLG/TPPS complex (Figure 5a and Table 1). Conversely, at $\text{pH} \geq 8$ irradiation of the complex produces a substantial lengthening of the fluorescence decay of the protein (Figure 5b). The deconvolution of the various decay components shows that the intermediate lifetime, τ_2 , lengthens by 130 ps at pH 8 and 260 ps at pH 9. At the same time the longer-lived component, τ_3 , lengthens

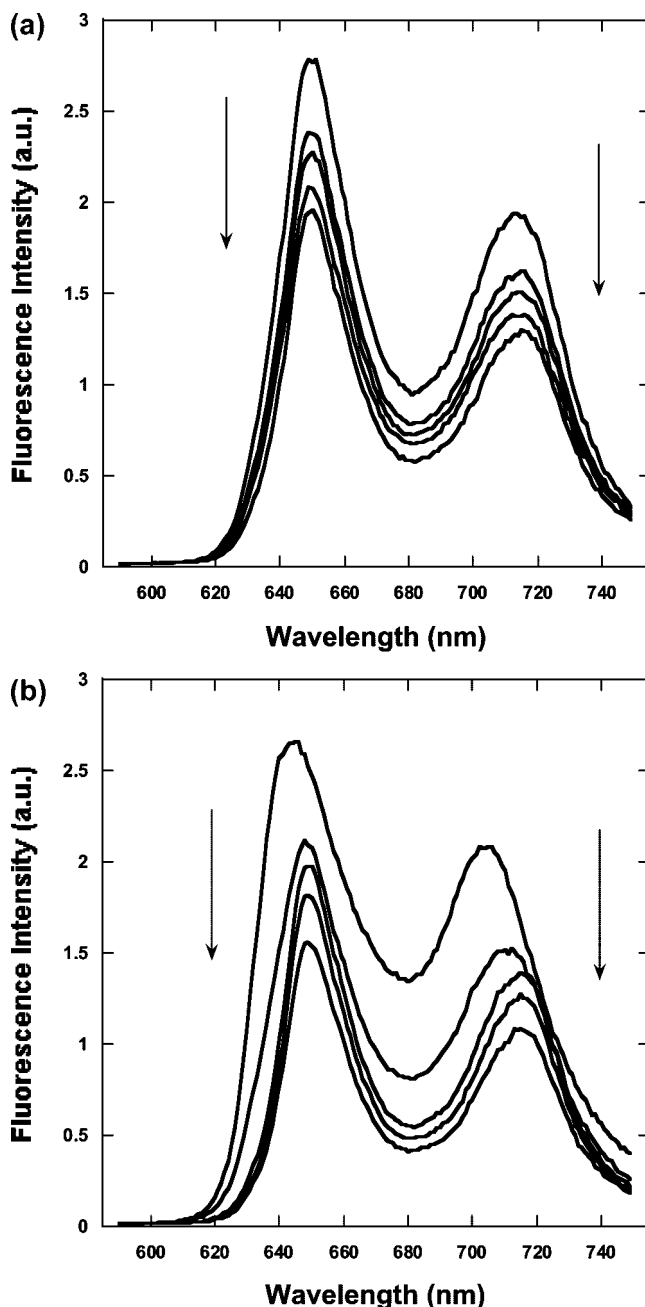


Figure 2. Emission spectra ($\lambda_{\text{ex}} = 413$ nm) of the porphyrin in the BLG/TPPS complex as a function of irradiation energy density (0.0, 0.3, 0.6, 1.2, 3.6 J/cm^2). The spectrum shows both $Q'(0,0)$ and $Q'(1,0)$ emission peaks and the arrows indicate the direction of the fluorescence intensity as a function of increasing irradiation energy density. (a) pH 6, air-saturated solutions; (b) pH 9, air-saturated solutions. The spectra at pH 6 are also representative of the spectra at pH 7, whereas the spectra at pH 9 are representative also of the spectra at pH 8.

nearly 1 ns at both pH values (Table 1). Simultaneously, the relative amplitude of the third component, α_3 , increases at the expense of the relative amplitude of the intermediate component, α_2 (Table 1). Conversely, the lifetime and amplitude of the subnanosecond component remain basically unaltered (Supporting Information).

In agreement with what was already observed in absorption and steady-state emission, deoxygenation of the samples did not produce any qualitative change in the effects of irradiation, thus unequivocally suggesting that the photoinduced changes of BLG do not depend on the presence of diffusing O_2 . As shown in Figure 5c, irradiation of deoxygenated solutions of

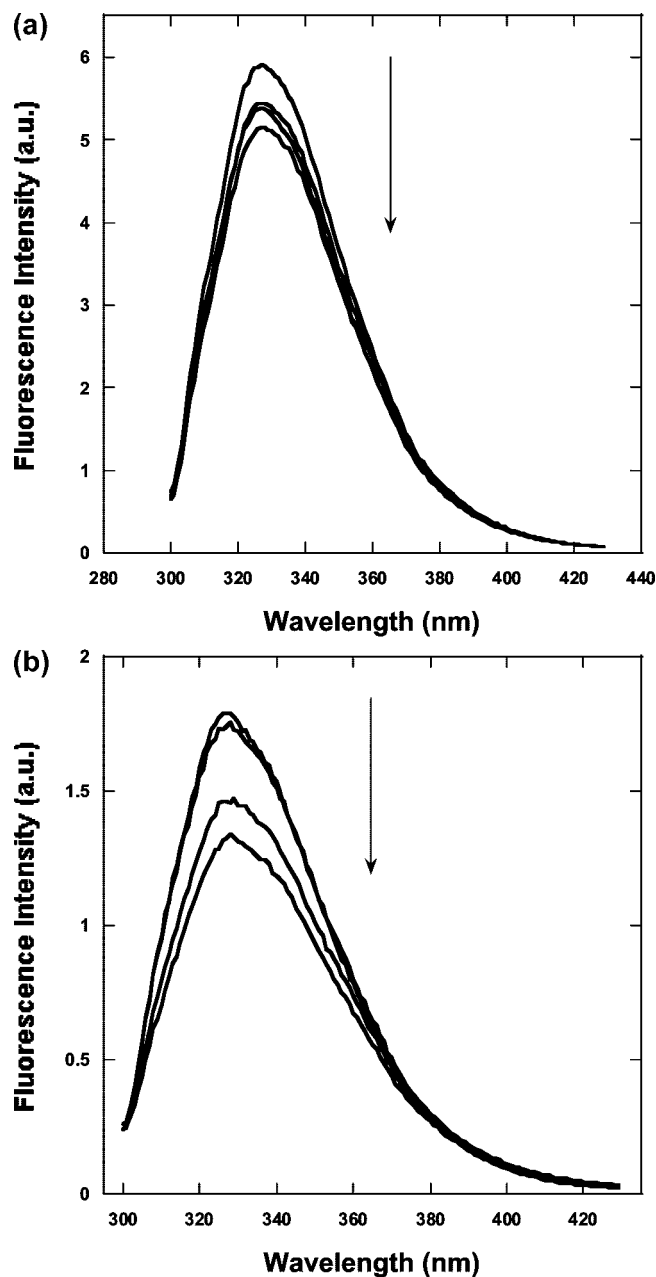


Figure 3. Emission spectra ($\lambda_{\text{ex}} = 295$ nm) of the protein in the BLG/TPPS complex as a function of irradiation energy density (0.0, 0.3, 0.6, 1.2, 3.6 J/cm²). (a) pH 6, air-saturated solutions; (b) pH 9, air-saturated solutions. The arrow indicates the direction of fluorescence intensity change at increasing irradiation energy density. The decrease in intensity does not produce a shift of the maximum. The spectra at pH 6 are also representative of the spectra at pH 7, whereas the spectra at pH 9 are representative also of the spectra at pH 8.

TPPS/BLG complex produced a lengthening of the emission decay of the protein which is comparable to the one in air (Table 1). The numerical values of the lifetimes (in particular τ_2 and τ_3) are larger in deoxygenated samples (for both irradiated and nonirradiated samples), according to the quenching that O₂ produces on the fluorescence of Trp residues in proteins.³⁴

The contribution of the emission band that appears at 405 nm after irradiation could not be investigated because the pulsed light sources available in our laboratory would excite a large contribution of the protein fluorescence even at an emission >400 nm.

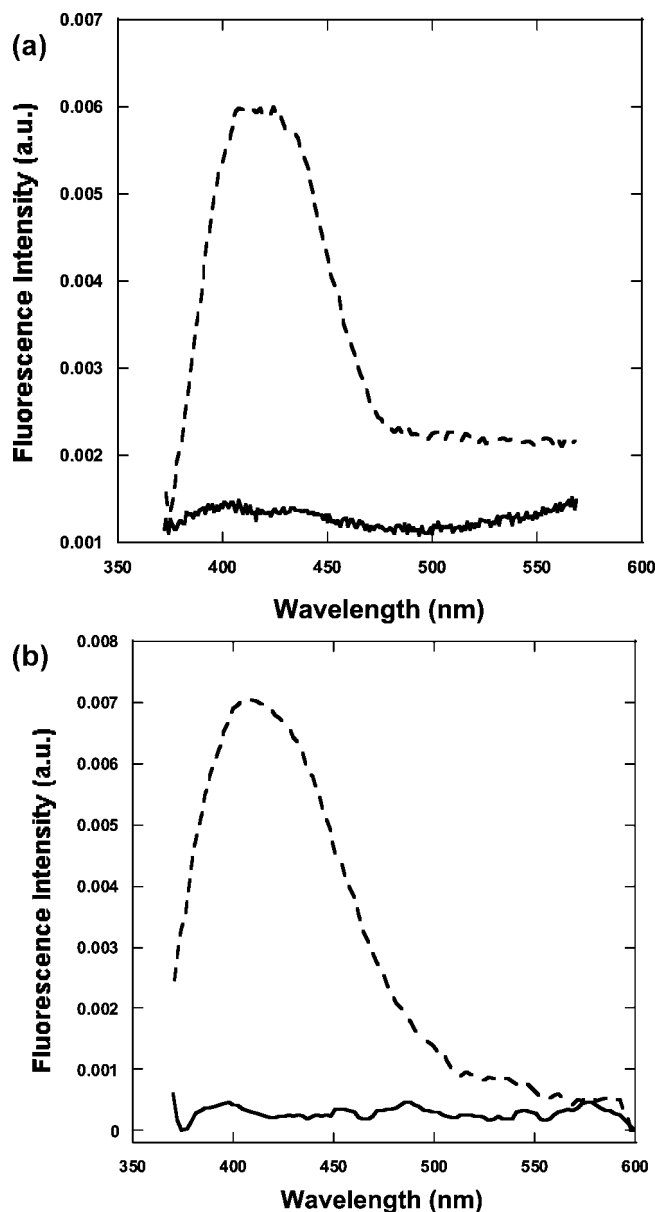


Figure 4. Emission spectra ($\lambda_{\text{ex}} = 320$ nm) of the nonirradiated (solid line) and irradiated (dashed line) BLG/TPPS complex. Energy density for the irradiated complex = 3.6 J/cm². (a) pH 6, air-saturated solutions; (b) pH 9, air-saturated solutions. The spectra at pH 6 are also representative of the spectra at pH 7, whereas the spectra at pH 9 are representative also of the spectra at pH 8.

Circular Dichroism in Air-Saturated Samples. 450–320 nm (TPPS). No CD activity can be observed for TPPS bound to BLG, in agreement with the fact that binding to BLG occurs without large distortions of the porphyrin ring.^{35,36} Irradiation of TPPS does not induce any CD activity of the porphyrin, indicating that photoinduced mechanisms between TPPS and BLG do not produce new optically active species of the porphyrin or distort its structure.

320–250 nm (Aromatic Amino Acids). The spectra show negative peaks at 286 and 293 nm due to Trp residues and other negative peaks between 280 and 260 nm due to Tyr residues^{37,38} (Figure 6a). At pH ≤ 7 irradiation of the complex prompts a small decrease in the CD negative intensity and a < 10% increase of the ratio between the negative peaks at 293 and 286 nm, in comparison with the nonirradiated complex as well as the irradiated and nonirradiated BLG. This indicates some changes in the Trp residues or in their interaction with proximal

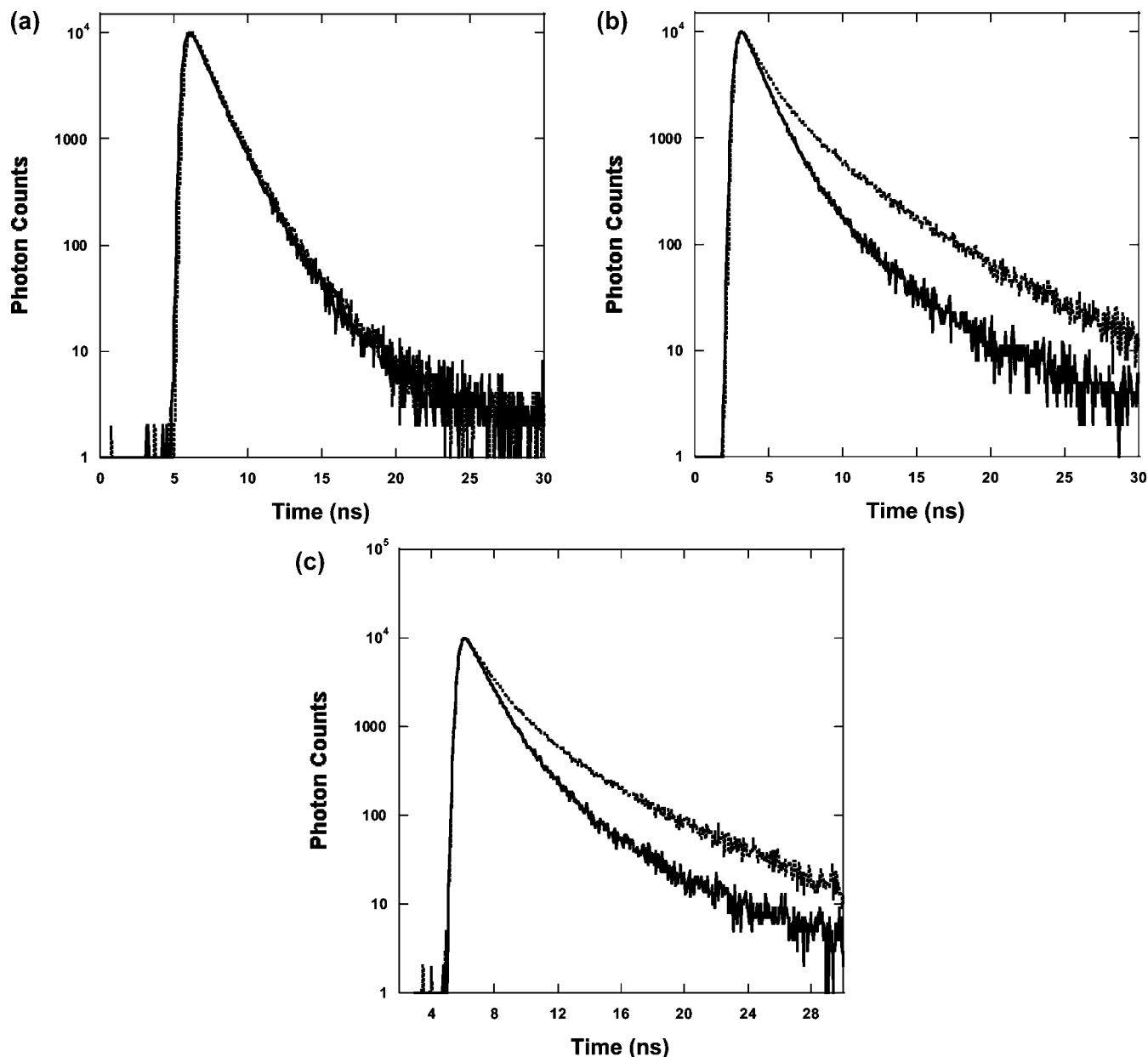


Figure 5. Fluorescence decay of the protein in the BLG/TPPS complex. $\lambda_{\text{ex}} = 295 \text{ nm}$, $\lambda_{\text{em}} = 330 \pm 4 \text{ nm}$. Solid line = nonirradiated complex; dotted line = complex irradiated with 3.6 J/cm^2 . (a) pH 6, air-saturated solution. (b) pH 9, air-saturated solution. (c) pH 9, deoxygenated solution.

groups. At alkaline pH however the difference is more dramatic. As Figure 6b shows, the signature double peak (293, 286 nm) of Trp residues decreases drastically while at the same time a broad peak centered near 321 nm appears (inset of Figure 6b). This is an indication that the Trp residues may have been chemically modified.

250–196 nm (Protein Backbone). *Before Irradiation.* The experiments only yielded quality data between 250 and 195 nm. Although this range excludes a portion of the spectrum important for the analysis of the secondary structure,³⁹ our analysis is comparable to the ones reported before for CD spectra at $\lambda > 200 \text{ nm}$.⁴⁰ First of all, it should be noted that the spectra of BLG (alone or in the complex) at alkaline pH are slightly different from the ones at pH 7 and below. Although the spectrum maintains largely the fingerprint of β -conformation ($>55\%$ between sheets and turns (Table 2)), a small shift to lower wavelengths at pH ≥ 8 (Figure 7a) indicates a slight, but above the experimental error, increase ($\sim 7\%$) in unordered

(random coil) at the expense of β -conformation (Table 2), as calculated with CDPro spectral analysis of the CD signal. This is an indication of a diminished stability of the protein at higher pH as it has been suggested in the past.^{25,41}

After Irradiation. Figure 7b shows that at pH ≤ 7 there is a nearly perfect overlap between the spectra of the protein and the complex before and after laser irradiation. This indicates that there are no extensive structural effects in BLG. At pH ≥ 8 , however, the spectra of the irradiated TPPS/BLG complex show a larger negative peak which shifts from 215 to 207 nm. Spectral analysis with CDPro reveals a large increase in the contribution of unordered structure (from 34% to 43%) and an overall decrease of the β -sheet + β -turn contribution (from 54% to 48%), while the contribution of the helices remains constant (Table 2). This effect is similar, but larger in scale, to the one shown by Qi et al.³⁹ for the unfolding of BLG at $T > 60^\circ \text{C}$.

No structural effect was observed upon irradiation (at 405 nm) of BLG in the absence of TPPS at any pH value.

TABLE 1: Summary of Fluorescence Decay Parameters of the Protein in the Irradiated BLG/TPPS Complex in Air and in N₂ ($\lambda_{\text{ex}} = 295$ nm, $\lambda_{\text{em}} = 330 \pm 4$ nm)^a

	0 (J)	0.3 (J/cm ²)	0.6 (J/cm ²)	1.2 (J/cm ²)	3.6 (J/cm ²)
pH 6					
α_2 (irr. air)	0.71 \pm 0.02	0.67 \pm 0.03	0.65 \pm 0.03	0.68 \pm 0.04	0.67 \pm 0.03
α_2 (irr. N ₂)	0.73 \pm 0.02	0.76 \pm 0.04	0.79 \pm 0.03	0.76 \pm 0.02	0.79 \pm 0.04
τ_2 (irr. air)	1.19 \pm 0.05	1.17 \pm 0.05	1.10 \pm 0.11	1.10 \pm 0.10	1.23 \pm 0.11
τ_2 (irr. N ₂)	1.31 \pm 0.06	1.39 \pm 0.10	1.32 \pm 0.12	1.33 \pm 0.06	1.35 \pm 0.01
α_3 (irr. air)	0.18 \pm 0.03	0.23 \pm 0.02	0.25 \pm 0.02	0.28 \pm 0.02	0.21 \pm 0.02
α_3 (irr. N ₂)	0.20 \pm 0.03	0.14 \pm 0.03	0.14 \pm 0.03	0.11 \pm 0.03	0.11 \pm 0.03
τ_3 (irr. air)	2.36 \pm 0.14	2.27 \pm 0.16	2.20 \pm 0.21	2.14 \pm 0.21	2.29 \pm 0.22
τ_3 (irr. N ₂)	2.48 \pm 0.09	2.61 \pm 0.13	2.54 \pm 0.20	2.53 \pm 0.20	2.52 \pm 0.09
pH 9					
α_2 (irr. air)	0.69 \pm 0.02	0.59 \pm 0.03	0.54 \pm 0.03	0.52 \pm 0.04	0.49 \pm 0.03
α_2 (irr. N ₂)	0.66 \pm 0.02	0.62 \pm 0.04	0.55 \pm 0.03	0.53 \pm 0.02	0.56 \pm 0.04
τ_2 (irr. air)	1.37 \pm 0.05	1.33 \pm 0.05	1.60 \pm 0.11	1.55 \pm 0.10	1.63 \pm 0.11
τ_2 (irr. N ₂)	1.37 \pm 0.06	1.50 \pm 0.10	1.59 \pm 0.12	1.64 \pm 0.06	1.65 \pm 0.01
α_3 (irr. air)	0.12 \pm 0.03	0.27 \pm 0.02	0.28 \pm 0.02	0.33 \pm 0.02	0.35 \pm 0.02
α_3 (irr. N ₂)	0.11 \pm 0.03	0.17 \pm 0.03	0.23 \pm 0.03	0.25 \pm 0.03	0.18 \pm 0.03
τ_3 (irr. air)	4.09 \pm 0.14	4.31 \pm 0.16	5.09 \pm 0.21	4.91 \pm 0.21	4.98 \pm 0.22
τ_3 (irr. N ₂)	4.22 \pm 0.09	4.73 \pm 0.13	4.99 \pm 0.20	5.04 \pm 0.20	5.06 \pm 0.09

^a Time-resolved fluorescence was analyzed with three decay components. Data in the table show only the decay parameters that are affected by irradiation. The complete set of parameters is available in the Supporting Information.

TABLE 2: Analysis of the CD Spectra of BLG and TPPS/BLG Complexes Using CDpro (CDSSTR, CONTNILL, SELCON)^a

	α (%)	β (%)	turn (%)	random (%)
pH 6 (air)				
BLG nonirradiated	0.106 \pm 0.06	0.375 \pm 0.08	0.205 \pm 0.02	0.312 \pm 0.06
BLG after irradiation	0.123 \pm 0.08	0.401 \pm 0.10	0.198 \pm 0.06	0.287 \pm 0.04
BLG/TPPS before irradiation	0.090 \pm 0.02	0.387 \pm 0.04	0.199 \pm 0.03	0.307 \pm 0.08
BLG/TPPS nonirradiated	0.087 \pm 0.03	0.375 \pm 0.04	0.203 \pm 0.04	0.303 \pm 0.09
BLG/TPPS after irradiation	0.092 \pm 0.04	0.361 \pm 0.04	0.201 \pm 0.05	0.308 \pm 0.06
pH 9 (air)				
BLG nonirradiated	0.073 \pm 0.03	0.363 \pm 0.06	0.196 \pm 0.03	0.334 \pm 0.16
BLG after irradiation	0.113 \pm 0.07	0.324 \pm 0.08	0.210 \pm 0.02	0.350 \pm 0.09
BLG/TPPS before irradiation	0.103 \pm 0.07	0.334 \pm 0.08	0.208 \pm 0.02	0.351 \pm 0.08
BLG/TPPS nonirradiated	0.117 \pm 0.08	0.338 \pm 0.05	0.205 \pm 0.02	0.339 \pm 0.09
BLG/TPPS after irradiation	0.100 \pm 0.06	0.285 \pm 0.06	0.180 \pm 0.02	0.432 \pm 0.03
pH 9 (nitrogen)				
BLG/TPPS before irradiation	0.110 \pm 0.07	0.335 \pm 0.08	0.210 \pm 0.02	0.341 \pm 0.08
BLG/TPPS nonirradiated	0.068 \pm 0.03	0.339 \pm 0.06	0.209 \pm 0.02	0.337 \pm 0.06
BLG/TPPS after irradiation	0.079 \pm 0.04	0.297 \pm 0.06	0.202 \pm 0.03	0.419 \pm 0.08

^a Data are presented as percentages of each secondary structure \pm SD.

Circular Dichroism in Deoxygenated Samples. In comparison with samples in air, eliminating O₂ from the solution does not produce any difference in the CD spectra regardless of the pH of the solution or the spectral range. However, our focus was to establish whether O₂ is necessary to prompt the large photoinduced CD changes observed in air at alkaline pH. As Figure 7d shows, the irradiation-induced conformational change of BLG in the complex still occurs to nearly the same extent as it does in air-saturated samples (Table 2). This result is in agreement with the fluorescence decay data and show that O₂ is not necessary to prompt the conformational rearrangement of the protein.

Capillary Liquid Chromatography–Mass Spectrometry (LC/MS) and –Tandem Mass Spectrometry (LC/MS/MS). The intact average mass of BLG, as determined by capillary LC/MS and maximum entropy deconvolution of the electrospray charge-state envelope, was 18 278 Da (Figure 8a). This is in excellent agreement, with less than a 1 Da or 55 ppm mass error, with the theoretical average mass of the amino acid sequence for gil6729725 (NCBI sequence database) at 18 277 Da (Figure 8a, inset). The charge-state envelope for BLG spanned from $[m + 20H]^{20+}$ to $[m + 10H]^{10+}$ with the most

abundant charge state ($[m + 15H]^{15+}$) at m/z 1219.5. The minor, unlabeled, peaks in Figure 8a correspond to an unknown protein impurity present at less than 10% the relative abundance of BLG in both nonirradiated and irradiated samples. The amino acid sequence of BLG, as determined by capillary LC/MS/MS of tryptic digests and probability-based protein database searching of MS/MS spectra,⁴² was identified as gil6729725 with 94% sequence coverage (Figure 8a, inset). Tryptic peptides with an MS/MS spectrum that could be assigned to BLG are shown in bold. Significantly, tryptic peptides spanning both Trp19 (underlined) and 61 were observed. Error tolerant protein database searching⁴³ of MS/MS spectra from capillary LC/MS/MS of tryptic digests of irradiated BLG samples showed a +19.99 Da modification of Trp19 to hydroxykynurenine (OHKyn) in a tryptic peptide spanning amino acid residues 15–40 (Figure 8b). The theoretical monoisotopic mass of the unmodified- and OHKyn-modified forms of this tryptic peptide is 2706.37 and 2726.36 Da, respectively. The observed monoisotopic mass of the OHKyn-modified tryptic peptide, with amino acid sequence VAGTW*YSLAMAASDISLLDAQSAPLR, was 2726.70 Da. This is in excellent agreement, with less than a 127 ppm (precursor ion) mass error, with the theoretical

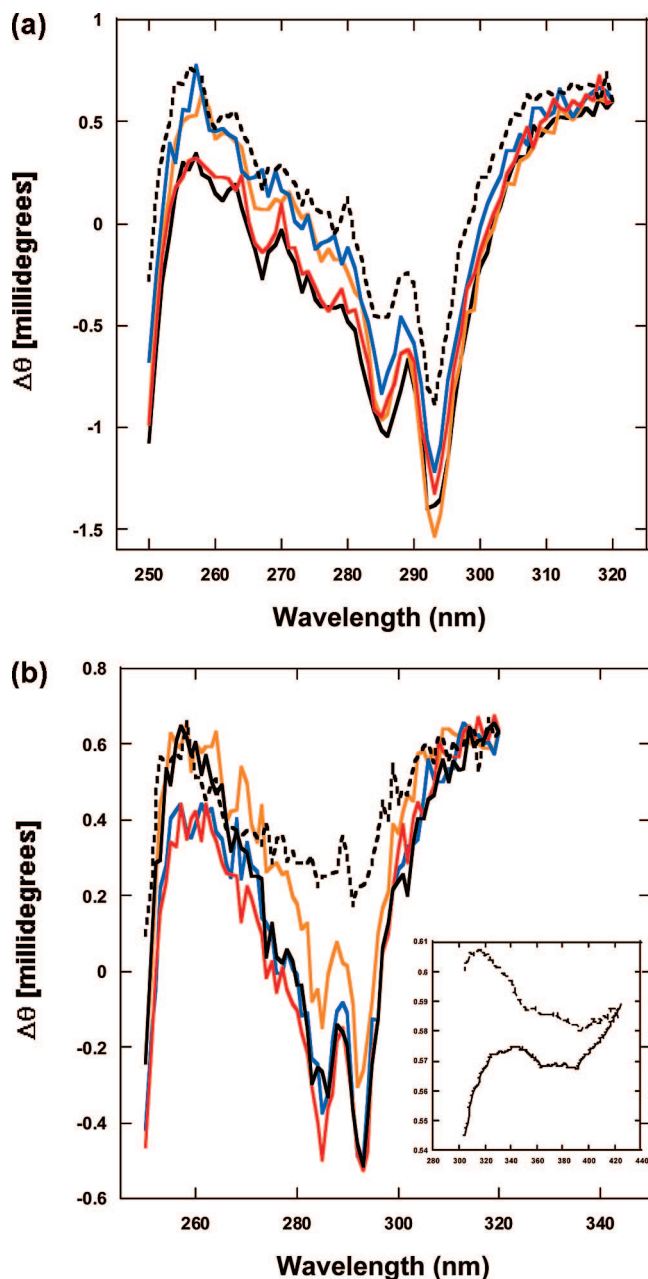


Figure 6. CD spectrum of the aromatic amino acids region (250–320 nm). Black solid = BLG/TPPS complex before irradiation; blue = BLG before irradiation; orange = BLG after irradiation (3.6 J/cm^2); red = BLG/TPPS complex nonirradiated; black dashed = BLG/TPPS complex after irradiation (3.6 J/cm^2). (a) pH 6, (b) pH 9. The inset in (b) is overlap of the spectra of the nonirradiated complex (solid) and the irradiated complex (dashed) in the 310–420 nm region of the photoproduct and the porphyrin.

monoisotopic mass. Likewise, the OHKyn assignment to Trp19 is in excellent agreement, with less than a 272 ppm (product ion rms) mass error, with the theoretical monoisotopic masses for gas-phase fragmentation (CID) of this OHKyn-modified tryptic peptide. Lastly, confidence in our MS/MS assignments is reflected by the low expectation values of 1.3×10^{-7} for this OHKyn-modified tryptic peptide, observation of 15 OHKyn-specific product ions, and observation of the oxidized-methionine form of this peptide (data not shown), respectively.

Discussion

Photoinduced Conformational Changes. Our experiments show that visible laser irradiation of the porphyrin in the

noncovalent TPPS/BLG complex is capable of triggering conformational changes of the protein. The changes can be summarized as a large unfolding of the β -structure (including turns) of the protein (Table 2). This indicates that the photoinduced mechanism breaks several hydrogen bonds that hold the β -sheets together. What is (or are) the mechanisms that can trigger the unfolding? One trivial explanation could be a thermal effect due to the conversion of absorbed light into heat by the porphyrin. However, the temperature of the solution does not change during irradiation. Moreover considering that the OD of the solutions at the laser's wavelength corresponds to $\sim 2 \text{ mW}$ of incident energy actually absorbed and that the concentration of TPPS is $\sim 1 \text{ } \mu\text{M}$, this leads to an average value of 140 ms between absorption events. This time is large compared to heat diffusion in water or even within the protein, and therefore, one can assume that there is no additive effect in temperature due to photon absorption because at the time a later photon is absorbed the localized temperature increase caused by the previous photon has already decayed back to room temperature.⁴⁴ Therefore, even if one assumes that the entire energy of one photon ($4.19 \times 10^{-19} \text{ J}$) absorbed by TPPS is converted into heat, this would correspond to a transient temperature change in the protein of $\sim 2 \text{ } ^\circ\text{C}$ (estimated assuming a constant heat capacity for BLG = $1.5 \text{ J K}^{-1} \text{ g}^{-1}$ ⁴⁵). Such temperature increase is not sufficient to cause a significant change in structure as the one observed for thermal denaturation of BLG.^{45,46} Furthermore, since the optical density of the sample and the laser power was the same at all pH values, one would expect thermal unfolding at all pH values since the ΔT required for thermal denaturation is $\gg 2 \text{ } ^\circ\text{C}$ at acidic as well as alkaline pH. On the contrary, TPPS-mediated unfolding occurs only at $\text{pH} \geq 8$. Thus, we rule out thermal denaturation.

If the effect is not thermal, one has to consider the possible photophysical/photochemical events that may prompt unfolding. The unfolding is prompted only at alkaline pH (Figure 7, Table 2), where the protein is less stable,^{25,41} and is accompanied by a red shift of the TPPS spectra (Figure 1, Figure 2, and Supporting Information), as well as of BLG emission (Figure 3b), and the lengthening of the fluorescence decay of the protein (Figure 5B). We believe these are all effects of a photoinduced change in the conformation of BLG in the complex. The TPPS-induced unfolding affects the region of Trp19 (which is the only Trp residue contributing to BLG fluorescence) and suggests an increased exposure of this residue to a polar environment. LC/MS confirms the modifications of Trp19 to OHKyn (Figure 8b); however, because of its spectral characteristics ($\lambda_{\text{max}}^{\text{abs}} = 321 \text{ nm}$; $\lambda_{\text{max}}^{\text{em}} = 408 \text{ nm}$), the contribution of the chemically modified Trp (Figures 1, 5, and 8b) to the fluorescence lifetime experiments ($\lambda_{\text{ex}} = 295 \text{ nm}$; $\lambda_{\text{em}} = 330 \text{ nm}$) are likely negligible. The unfolding of BLG does not cause TPPS to detach from the protein. If such an effect occurred, the fluorescence of TPPS would shift to shorter wavelengths (due to the increase of free base TPPS). In fact, the opposite occurs (Figure 1b,c and Figure 2b). These results are consistent with an even stronger interaction (lower energy) with between the porphyrin ligand and BLG which could be due to an increased accommodation of the hydrophobic porphyrin ring within a less rigid BLG or a stronger Coulomb interaction, due to reduced distance between the SO_3^- groups in TPPS and the positively charged Lys and Arg residues to which the porphyrin docks.⁴⁷

A remarkable result gathered from our experiments is that the unfolding of BLG occurs via O_2 -independent mechanisms. The observed photoinduced unfolding occurs in N_2 -saturated solutions to the same extent as it does in air-saturated solutions;

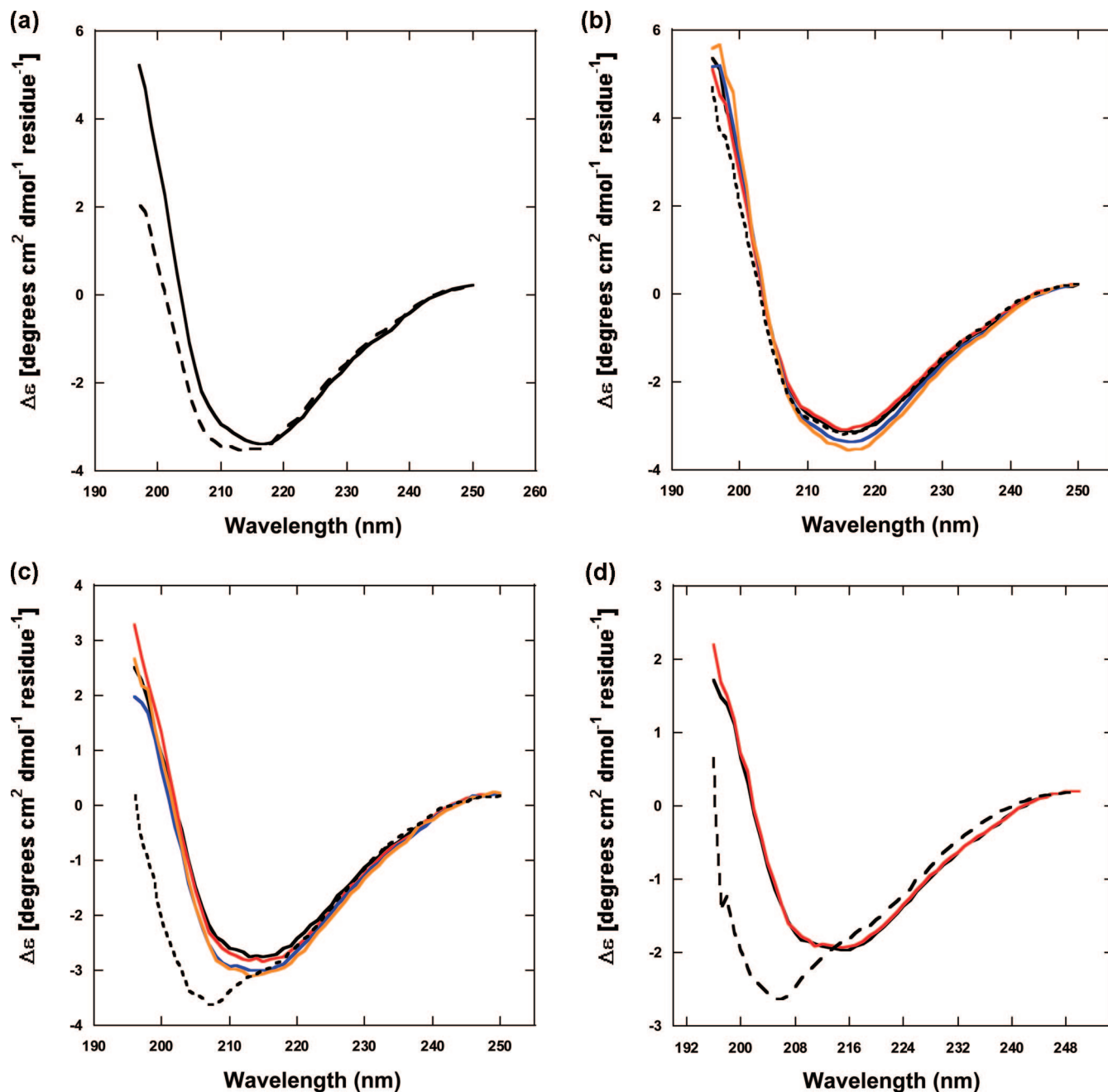


Figure 7. CD spectra in the region of the secondary structure of the protein (195–250 nm). (a) Spectra of BLG at pH 6 (solid) and pH 9 (dashed). (b) Comparison of spectra at pH 6, air-saturated solutions. Black solid = BLG/TPPS complex before irradiation; blue = BLG before irradiation; orange = BLG after irradiation (3.6 J/cm²); red = BLG/TPPS complex nonirradiated; black dashed = BLG/TPPS complex after irradiation (3.6 J/cm²). (c) Comparison of spectra at pH 9, air-saturated solutions. The color scheme is the same as for (b). (d) Comparison of spectra at pH 9, N₂-saturated solutions. Black solid = BLG/TPPS complex before irradiation; red = BLG/TPPS complex nonirradiated; black dashed = BLG/TPPS complex after irradiation (3.6 J/cm²).

thus mechanisms that involve ROS are not responsible for BLG unfolding. This is surprising because porphyrin-mediated photosensitization has typically been attributed to their large yield for triplet state-sensitized singlet oxygen (¹O₂) or the formation of other ROS.²² These mechanisms are also commonly accepted as the major, if not the exclusive, contributors to the biomedical applications of porphyrins.¹⁷ However, our results suggest a new possibility for the mechanisms triggered by porphyrins interacting with biomolecules: an O₂-independent, type III photosensitization.

Absorption, fluorescence spectroscopy and LC/MS provide additional evidence for our interpretation. Absorption (Figure 1) and emission spectra (Figure 2) did not reveal the presence

of TPPS photoproducts. LC/MS also ruled out the presence of TPPS photoproduct or the formation of cross-links between BLG and the porphyrin. Indeed, the intact average mass of nonirradiated and irradiated samples is in excellent agreement with the theoretical value for unmodified BLG. Nevertheless, the decrease of absorption and emission intensities indicates a depletion of the porphyrin ground-state and suggests a reaction with BLG. Such reaction occurs at all pH values as the effects of irradiation ((i) the bleaching of BLG absorption (Figure 1), (ii) the simultaneous appearance of the shoulder at 320 nm (Figure 1) and its emission band at 405 nm (Figure 5), as well as (iii) the decrease of the CD signal in the aromatic amino acid region (Figure 7, a and b)) occur at all pH values, even if

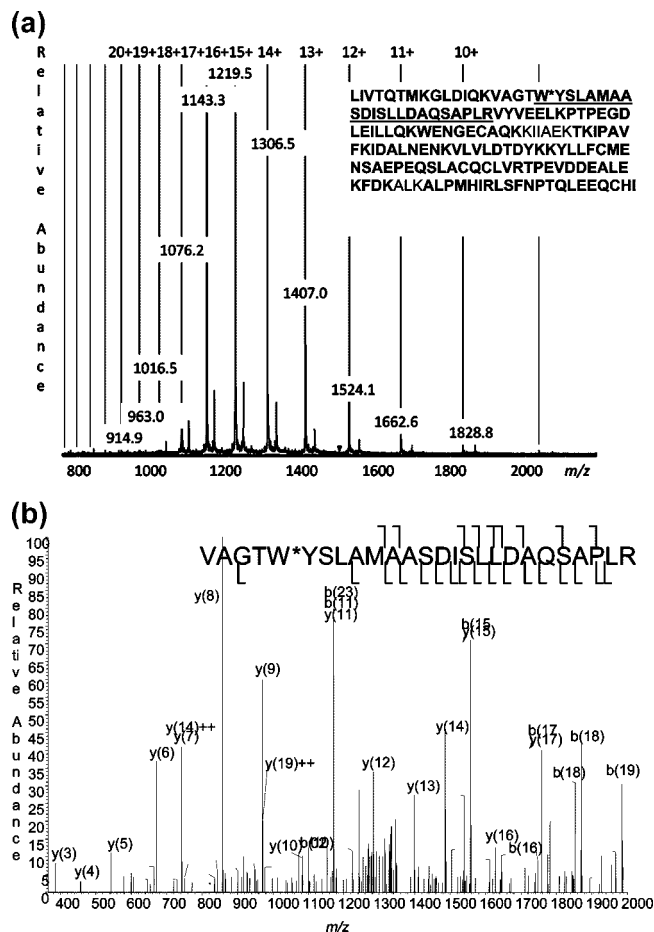
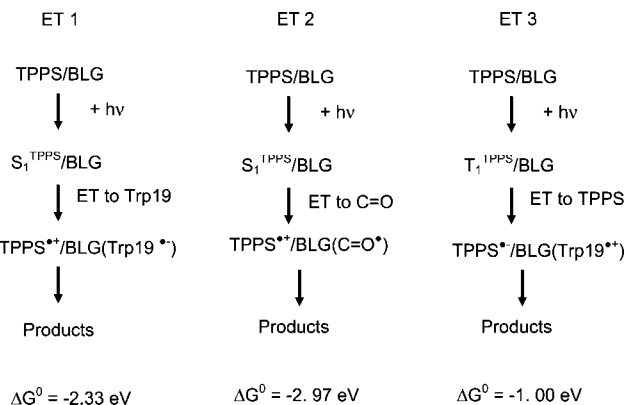


Figure 8. (a) Intact average mass of BLG, as determined by capillary LC/MS and maximum entropy deconvolution of the electrospray charge-state envelope, was 18 278 Da. This is in excellent agreement with the theoretical average mass of the amino acid sequence for gil6729725 at 18 277 Da (inset). (b) Error tolerant protein database searching of MS/MS spectra from capillary LC/MS/MS of tryptic digests of irradiated BLG samples showed a +19.99 Da modification of tryptophan 19 to hydroxykynurenine (OHKyn) in a tryptic peptide spanning amino acid residues 15–40. The observed monoisotopic mass of this OHKyn-modified tryptic peptide, with amino acid sequence VAGTW*YSLAMAA, SDISLLDAQSAPLR, was 2726.70 Da. This is in excellent agreement with the theoretical monoisotopic mass. Likewise, the OHKyn assignment to Trp19 is in excellent agreement with the theoretical monoisotopic masses for gas-phase fragmentation of this OHKyn-modified tryptic peptide.

unfolding of BLG does not occur (Figure 8b). The only difference is that at $\text{pH} \geq 8$ the effects listed above are larger. On the basis of this evidence, we conclude that the same mechanism(s) responsible for the unfolding of BLG occurs at all pH values but that only at $\text{pH} \geq 8$ these changes effectively prompt the conformational rearrangement of the protein. Why would the pH be the deciding factor of whether BLG is unfolded after the irradiation of the attached porphyrin? The pH effect could be due to a higher efficiency of the photochemical mechanisms responsible for prompting the unfolding; more likely, though, the unfolding could be prompted by the documented larger instability of BLG at alkaline pH.^{41,48}

The last piece of the puzzle is provided by LC/MS/MS which reveals the presence of a low abundance OHKyn modification of Trp19 (Figure 8b) which is also evident in the spectroscopic data (Figures 1, 5, and 7b).⁴⁹ Typically, kynurenines are oxidation products of indole moieties, however our data show that, in this case OHKyn could be formed also in the absence

SCHEME 1



of O_2 . Indeed, some studies have reported the formation of kynurenines under anaerobic conditions.⁵⁰ The O_2 independence of the spectroscopic data and the formation of OHKyn suggest that the initial photoinduced mechanism responsible for the unfolding of BLG is a charge transfer. Three possible mechanisms are likely for TPPS bound to BLG: (1) direct photoinduced electron transfer (PET) from the excited singlet state of TPPS (S_1^{TPPS}) to the ground state of Trp19 (G_{Trp}), (2) PET from S_1^{TPPS} to the ground state of the carbonyl group of a proximal peptide bond ($G_{\text{C=O}}$), or (3) PET from the Trp residue (G_{Trp}) to the excited triplet state of TPPS (T_1^{TPPS}) (Scheme 1). Using the Rehm–Weller equation and available redox potential of the various ground- and excited-state species,^{51–53} we estimated that direct PET is energetically favorable for all three mechanisms. However, the $S_1^{\text{TPPS}} \rightarrow G_{\text{C=O}}$ ET is more favorable by $>0.60 \text{ eV}$ with respect to $S_1^{\text{TPPS}} \rightarrow G_{\text{Trp}}$ ET ($\Delta G^0 = -2.97 \text{ eV}$ vs $\Delta G^0 = -2.33 \text{ eV}$). It is therefore more likely that PET proceeds from S_1^{TPPS} to an adjacent C=O (peptide bond) than to Trp. The likelihood of PET to a C=O group is made larger by the location of TPPS on BLG which places the porphyrin ring in closer proximity to several peptide bonds than to Trp19.¹² Direct oxidation of Trp19 (which would more easily explain the formation of OHKyn) could proceed via $G_{\text{Trp}} \rightarrow T_1^{\text{TPPS}}$ ET for which $\Delta G^0 = -1.00 \text{ eV}$.^{51,54} Such contribution is still energetically favorable but an estimate, using the Marcus theory⁵⁵ with the combined value of ΔG^0 and distance between donor and acceptor,⁴⁷ would yield a rate of PET for $G_{\text{Trp}} \rightarrow T_1^{\text{TPPS}}$ which is approximately 2% of the magnitude of the rate for $S_1^{\text{TPPS}} \rightarrow G_{\text{C=O}}$. Thus, we think that $S_1^{\text{TPPS}} \rightarrow G_{\text{C=O}}$ PET is the mechanism that, either directly or through migration to other peptide bonds, destabilizes hydrogen bonds in some of the β -sheets and β -turns and prompts the partial unfolding of BLG. This is not unprecedented since other protein/chromophore systems were shown to produce large conformational changes of proteins via charge transfer at the chromophore site.^{56,57} The charge-induced partial unfolding of BLG would be favored at $\text{pH} \geq 8$ because at alkaline pH this protein has lower stability. The issue of the BLG instability at alkaline pH is being investigated by additional ongoing studies of the effects of the solution's temperature on the conformational changes induced by the irradiation of the noncovalently attached porphyrin. Increasing the temperature of the solution would destabilize the protein so that the TPPS-induced conformational changes could potentially occur also at acidic pH.

Conclusions

In conclusion, we have demonstrated that TPPS, noncovalently attached to a small globular protein (BLG), is capable

of mediating photoinduced unfolding of the polypeptide. The unfolding is large (~20%) and proceeds through PET between the porphyrin and the protein. This mechanism does not require the mediation of O₂ to produce molecular "damage" to the protein and can be categorized as a type III photosensitization mechanism. Additional investigations are ongoing; however, these results suggest that this property of TPPS can be translated to other porphyrin/protein systems and could be used to prompt photoinduced protein unfolding and protein inactivation as a viable strategy for biomedical applications of porphyrins.

Acknowledgment. The study was funded in part by a Faculty Research Award from the University of Texas at San Antonio (to L.B.) and by the AFRL/HE grant FA8650-07-1-6850 (to L.B.). For the duration of the project N.F.F. received MARC U*STAR support (NIH/NIGMS GM07717). J.B. is a TRIO McNair scholar and has been supported in part by a TRIO McNair Scholarship. The LC/MS experiments were carried out at the RCMi Proteomics Core at UTSA (NIH G12 RR013646). We thank Ms. Sruthi Eedala of the RCMi Proteomics Core for assistance with experiment design, sample preparation, data collection, results interpretation, and manuscript preparation.

Note Added after Print Publication. This paper was published on the Web on April 7, 2009, and in the April 30, 2009, issue. Due to a production error, Lorenzo Brancalion's name was misspelled. The electronic version was corrected and reposted to the Web issue on May 28, 2009. An Addition and Correction was also published (Belcher et al. *J. Phys. Chem. B* **2009**, *113*, DOI: 10.1021/jp904688t).

Supporting Information Available: Table of BLG fluorescence decay parameters at all pH values of irradiated vs nonirradiated BLG/TPPS complex; spectra of TPPS and the BLG/TPPS complex. This material is available free of charge via the Internet at <http://pubs.acs.org>.

References and Notes

- Muñoz, V. *Annu. Rev. Biophys. Biomol. Struct.* **2007**, *36*, 395.
- Abbruzzetti, S.; Sottini, S.; Viappiani, C.; Corrie, J. E. *Photochem. Photobiol. Sci.* **2006**, *5*, 621.
- Eaton, W. A.; Munoz, V.; Hagen, S. J.; Jas, G. S.; Lapidus, L. J.; Henry, E. R.; Hofrichter, J. *Annu. Rev. Biophys. Biomol. Struct.* **2000**, *29*, 327.
- Kubelka, J.; Hofrichter, J.; Eaton, W. A. *Curr. Opin. Struct. Biol.* **2004**, *14*, 76.
- Thompson, P. A.; Eaton, W. A.; Hofrichter, J. *Biophys. J.* **1996**, *70*, A177.
- Loweneck, M.; Milbradt, A. G.; Root, C.; Satzger, H.; Zinth, W.; Moroder, L.; Renner, C. *Biophys. J.* **2006**, *90*, 2099.
- Lee Jr, C. T.; Smith, K. A.; Hatton, T. A. *Biochemistry* **2005**, *44*, 524.
- Cheung, Y. L.; Puddicombe, S. M.; Gray, T. J.; Ioannides, C. *Carcinogenesis* **1994**, *15*, 1257.
- Kriegel, J. M.; Forster, F. K.; Nienhaus, G. U. *Biophys. J.* **2003**, *85*, 1851.
- Katona, G.; Snijder, A.; Gourdon, P.; Andreasson, U.; Hansson, O.; Andreasson, L. E.; Neutze, R. *Nat. Struct. Mol. Biol.* **2005**, *12*, 630.
- Lang, K.; Mosinger, J.; Wagnerova, D. M. *Coord. Chem. Rev.* **2004**, *248*, 321.
- Tian, F.; Johnson, E. M.; Zamarripa, M.; Sansone, S.; Brancalion, L. *Biomacromol.* **2007**, *8*, 3767.
- Brancalion, L.; Moseley, H. *Biophys. Chem.* **2002**, *96*, 77.
- Andrade, S. M.; Costa, S. M. B. *Biophys. J.* **2002**, *82*, 1607.
- Kenoth, R.; Reddy, D. R.; Maiya, B. G.; Swamy, M. J. *Eur. J. Biochem.* **2001**, 268.
- Morgan, W. T.; Smith, A.; Koskelo, P. *Biochim. Biophys. Acta* **1980**, *624*, 271.
- Sibata, C. H.; Colussi, V. C.; Oleinick, N. L.; Kinsella, T. J. *Braz. J. Med. Biol. Res.* **2000**, *33*, 869.
- Castano, A. P.; Mroz, P.; Hamblin, M. R. *Nat. Rev. Cancer* **2006**, *6*, 535.
- Tsaytler, P. A.; O'Flaherty, M. C.; Sakharov, D. V.; Krijgsvel, J.; Egmond, M. R. *J. Proteome Res.* **2008**, *7*, 3868.
- Kessel, D.; Castelli, M. *Photochem. Photobiol.* **2001**, *74*, 318.
- Xue, L. Y.; Chiu, S. M.; Fiebig, A.; Andrews, D. W.; Oleinick, N. L. *Oncogene* **2003**, *22*, 9197.
- Laustriat, G. *Biochimie* **1986**, *68*, 771.
- Fernandez, N. F.; Sansone, S.; Mazzini, A.; Brancalion, L. *J. Phys. Chem. B* **2008**, *112*, 7592.
- Lee, Jr., C. T.; Wang, S. C.; Hamill, A. C. *Biochemistry* **2007**, *46*, 7694.
- Qin, B. Y.; Bewley, M. C.; Creamer, L. K.; Baker, H. M.; Baker, E. N.; Jameson, G. B. *Biochemistry* **1998**, *37*, 14014.
- Girotti, A. W. *Biochim. Biophys. Acta* **1980**, *602*, 45.
- Tanford, C.; Bunville, L. G.; Nozaki, Y. *J. Am. Chem. Soc.* **1959**, *81*, 4032.
- Lakowicz, J. R. *Principles of Fluorescence Spectroscopy*, 3rd ed.; Springer: New York, 2006.
- Durbin, J.; Watson, G. S. *Biometrika* **1951**, *38*, 159.
- Greenfield, N. J. *Nat. Protoc.* **2006**, *1*, 2876.
- Sreerama, N.; Woody, R. W. *Anal. Biochem.* **2000**, *287*, 252.
- Sreerama, N.; Woody, R. W. *Anal. Biochem.* **2003**, *329*, 32–44.
- Harvey, B. J.; Bell, E.; Brancalion, L. *J. Phys. Chem. B* **2007**, *111*, 2610.
- Eftink, M. R.; Ghiron, C. A. *Anal. Biochem.* **1981**, *114*, 189.
- Pasternack, R. F. *Chirality* **2003**, *15*, 329–332.
- Kurtan, T.; Nesnas, N.; Koehn, F. E.; Li, Y. Q.; Nakanishi, K.; Berova, N. *J. Am. Chem. Soc.* **2001**, *123*, 5974.
- Rasmussen, P.; Barbiroli, A.; Bonomi, F.; Faoro, F.; Ferranti, P.; Iriti, M.; Picariello, G.; Iametti, S. *Biopolymers* **2007**, *86*, 57.
- Zhang, X.; Keiderling, T. A. *Biochemistry* **2006**, *45*, 8444.
- Qi, X. L.; Holt, C.; McNulty, D.; Clarke, D. T.; Brownlow, S.; Jones, G. R. *Biochem. J.* **1997**, *324*, 341.
- Crougennec, T.; Molle, D.; Mehra, R.; Bouhallab, S. *Protein Sci.* **2004**, *13*, 1340.
- Taulier, N.; Chalikian, T. V. *J. Mol. Biol.* **2001**, *314*, 873.
- Perkins, D. N.; Pappin, D. J.; Creasy, D. M.; Cottrell, J. S. *Electrophoresis* **1999**, *20*, 3551.
- Creasy, D. M.; Cottrell, J. S. *Proteomics* **2002**, *2*, 1426.
- James, D. W. *J. Material Sci.* **1968**, *3*, 540.
- Griko, Y. V.; Privalov, P. L. *Biochemistry* **1992**, *31*, 8810–8815.
- Qi, X. L.; Brownlow, S.; Holt, C.; Sellers, P. *Biochim. Biophys. Acta* **1995**, *1248*, 43.
- Silva, I.; Sansone, S.; Brancalion, L. *Protein J.* **2009**, *28*, 1.
- Casal, H. L.; Kohler, U.; Mantsch, H. H. *Biochim. Biophys. Acta* **1988**, *957*, 11.
- Pileni, M. P.; Wairant, P.; Santus, R. *J. Phys. Chem.* **1976**, *80*, 1804.
- Creed, D. *Photochem. Photobiol.* **1984**, *39*, 537.
- Harriman, A. *J. Phys. Chem.* **1987**, *91*, 6102.
- Chen, F. C.; Ho, J. H.; Chen, C. Y.; Su, Y. O.; Ho, T. I. *J. Electroanal. Chem.* **2001**, *499*, 17.
- D'Souza, F.; Deviprasad, G. R.; Hsieh, Y. Y. *Chem. Commun.* **1997**, 1997, 533.
- Tan, S.; Su, B.; Roussel, C.; Girault, H. H. *Inorg. Chim. Acta* **2008**, *361*, 746.
- Marcus, R. A.; Sutin, N. *Biochim. Biophys. Acta* **1985**, *811*, 265.
- Yang, H.; Luo, G.; Karnchanaphanurach, P.; Louie, T.-M.; Rech, I.; Cova, S.; Xun, L.; Xie, X. S. *Science* **2003**, *302*, 262.
- Xie, A.; Kelemen, L.; Hendriks, J.; White, B. J.; Hellingwerf, K. J.; Hoff, W. D. *Biochemistry* **2001**, *40*, 1510.

JP900957D